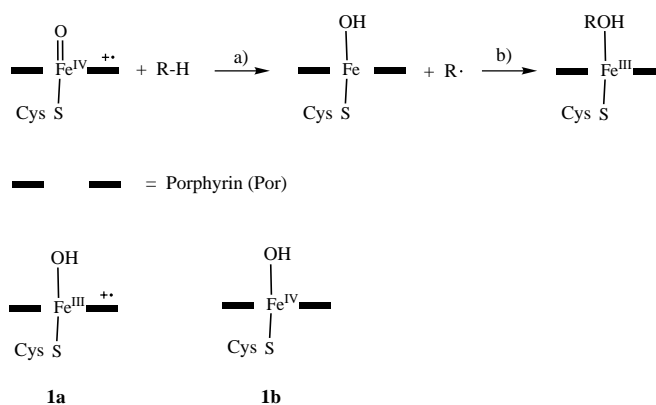


- [1] C. T. Kresge, M. E. Leonowicz, W. J. Roth, J. C. Vartuli, J. S. Beck, *Nature* **1992**, 359, 710.
- [2] T. Yanagisawa, T. Shimizu, K. Kuroda, C. Kato, *Bull. Chem. Soc. Jpn.* **1990**, 63, 988.
- [3] K. Moller, T. Bein, *Chem. Mater.* **1998**, 10, 2950.
- [4] D. M. Antonelli, J. Y. Ying, *Angew. Chem.* **1996**, 108, 461; *Angew. Chem. Int. Ed. Engl.* **1996**, 35, 426.
- [5] T. Sun, J. Y. Ying, *Nature* **1997** 389, 704.
- [6] H. Fujii, M. Ohtaki, K. Eguchi, *J. Am. Chem. Soc.* **1998**, 120, 6832.
- [7] V. F. Stone, Jr., R. J. Davis, *Chem. Mater.* **1998**, 10, 1468.
- [8] M. Yada, M. Machida, T. Kijima, *Chem. Commun.* **1996**, 769.
- [9] M. Yada, H. Hiyoshi, K. Ohe, M. Machida, T. Kijima, *Inorg. Chem.* **1997**, 36, 5565.
- [10] M. Yada, H. Kitamura, M. Machida, T. Kijima, *Langmuir* **1997**, 13, 5252.
- [11] M. Yada, H. Kitamura, M. Machida, T. Kijima, *J. Porous Mater.* **1998**, 5, 133.
- [12] M. Yada, H. Takenaka, M. Machida, T. Kijima, *J. Chem. Soc. Dalton Trans.* **1998**, 1547.
- [13] M. Yada, H. Kitamura, M. Machida, T. Kijima, *Inorg. Chem.* **1998**, 37, 6470.
- [14] M. Yada, M. Ohya, M. Machida, T. Kijima, *Chem. Commun.* **1998**, 1941.
- [15] M. Yada, M. Ohya, M. Machida, T. Kijima, unpublished results.
- [16] A. Chenite, Y. L. Page, V. R. Karra, A. Sayari, *Chem. Commun.* **1996**, 413.
- [17] G. S. Attard, J. C. Glyde, C. G. Goltner, *Nature* **1995**, 378, 366.
- [18] Y. Huang, W. M. H. Sachtleir, *Chem. Commun.* **1997**, 1181.
- [19] V. M. Goldschmidt, F. Ulrich, T. Barth, *Skr. Nor. Vidensk. Akad. Kl. I* **1925**, 5, 1.
- [20] I. Warshaw, R. Roy, *J. Phys. Chem.* **1961**, 65, 2048.
- [21] B. T. Holland, P. K. Isbester, C. F. Blanford, E. J. Munson, A. Stein, *J. Am. Chem. Soc.* **1997**, 119, 6796.
- [22] S. Brunauer, P. H. Emmett, E. Teller, *J. Am. Chem. Soc.* **1938**, 60, 309.
- [23] R. W. Cranston, F. A. Inkley, *Adv. Catal.* **1957**, 9, 143.

## On the “Rebound” Mechanism of Alkane Hydroxylation by Cytochrome P450: Electronic Structure of the Intermediate and the Electron Transfer Character in the Rebound Step\*\*

Michael Filatov, Nathan Harris, and Sason Shaik\*

Alkane hydroxylation is a key process by which the heme enzyme cytochrome P450 metabolizes xenobiotics.<sup>[1]</sup> The consensus mechanism (Scheme 1), called the rebound mechanism,<sup>[2]</sup> proceeds by an initial hydrogen abstraction from the alkane (RH) by the active ferryl–oxene species (Por<sup>+</sup>Fe<sup>IV</sup>=O), to form a radical R<sup>•</sup> and a hydroxo–iron complex as intermediates (step a). Subsequently the radical rebounds on the hydroxy group and generates the ferric–alcohol complex (step b). This mechanism is currently under



Scheme 1. Schematic representation of the rebound mechanism, and of the two electromeric forms (**1a** and **1b**) of the hydroxo–iron intermediate.

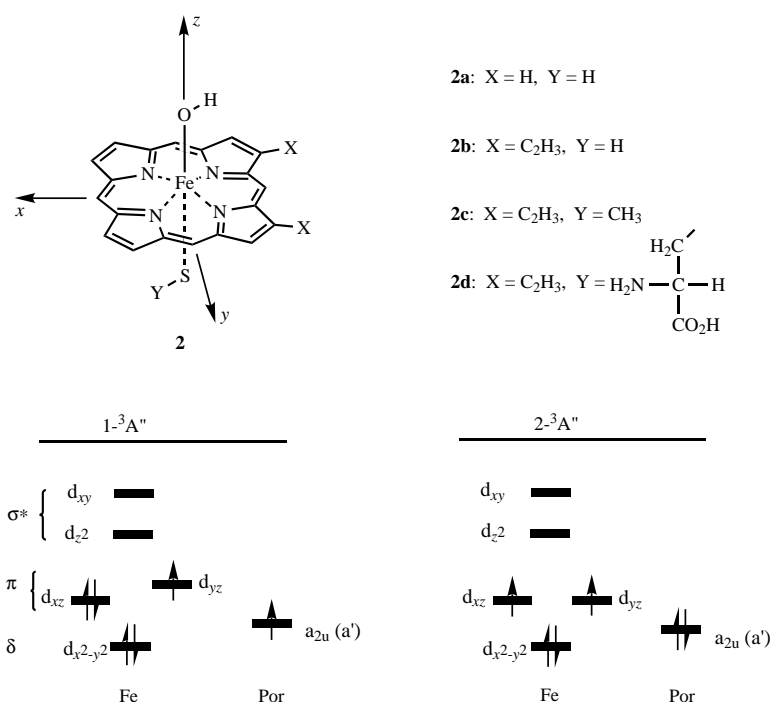
debate due to recent mechanistic studies,<sup>[3]</sup> using ultrafast radical clocks to probe the presence of a free radical, that suggest a concerted oxene-insertion mechanism. Nevertheless, quite a few investigations do report results which are consistent with the rebound mechanism.<sup>[2, 4]</sup> As such, the mechanism of a very important reaction in the vital system remains not fully resolved.

A great deal of mechanistic research has traditionally focused on whether the radical intermediate exists or not, while very few studies have addressed the nature of the hydroxo–iron species **1** (Scheme 1).<sup>[5]</sup> It is important to address the electronic structure of this intermediate, since this has bearing on its reactivity in the rebound step, and hence on an eventual resolution of the mechanistic dilemma as a whole. The ferryl–hydroxo species may exist in two electromeric<sup>[6]</sup> forms. In one (**1a**, Scheme 1) the iron appears as a Fe<sup>III</sup> center to provide a cation radical porphyrin, while the other (**1b**) contains high-valent Fe<sup>IV</sup> with a neutral porphyrin.<sup>[5, 7]</sup> The spin state of the complex may be low ( $S=1$ ), intermediate ( $S=2$ ), or high ( $S=3$ ).<sup>[7c]</sup> In addition, due to available alternative occupation modes of the d-orbital block, and of the porphyrin's orbitals (the  $a_{1u}$  and  $a_{2u}$  types<sup>[8]</sup>), there might exist a few closely lying states with different state symmetries. The present paper uses density functional and model solvent calculations to resolve this complex state situation for the hydroxo–iron species, and addresses due implications on the rebound mechanism.

All calculation were performed by use of the JAGUAR 3.5 package.<sup>[9]</sup> Benchmark calculations showed that the pure density functional BP86<sup>[10a]</sup> and the hybrid (HF/DFT) functional B3LYP levels<sup>[10b]</sup> give the same stability ordering for the two electromers, and therefore the rest of the study was performed with B3LYP. Based on previous experience with the oxo iron porphyrin,<sup>[8]</sup> reliable spin state ordering of organometallic species can be obtained with moderate basis sets, but geometry optimization is essential since different spin situations may have very different bond lengths between iron and the axial ligands. On iron we used the Los Alamos effective core potential coupled with the double zeta LACVP basis set,<sup>[11]</sup> while for the rest of the atoms we utilized the 6-31G basis set. The latter basis set was ascertained against a calculation that used the more flexible LACV3P basis set<sup>[11]</sup>

[\*] Prof. S. Shaik, Dr. M. Filatov, Dr. N. Harris  
Department of Organic Chemistry and  
The Lise Meitner-Minerva Center for  
Computational Quantum Chemistry  
Hebrew University, 91904 Jerusalem (Israel)  
Fax: (+972) 2-6585345  
E-mail: sason@yfaat.ch.huji.ac.il

[\*\*] This research was sponsored by the Volkswagen Stiftung and The Israeli Science Foundation (ISF). S.S. thanks the Humboldt Foundation for a Senior Research Award.



Scheme 2. Model species for the hydroxo-iron intermediate, and orbital diagrams for the electromeric forms 1-<sup>3</sup>A'' and 2-<sup>3</sup>A'' (see Table 1).

on iron and 6-311G(d) basis sets on C, N, and H, and which gave the same state ordering for **2a** (Scheme 2).

Scheme 2 shows the species used to model the hydroxo-iron complex. These range from the simplest model (**2a**) to more realistic ones that involve vinyl substituents at the  $\beta$ -pyrrole positions (as in the native protoporphyrin IX), and a cysteinato axial ligand (**2d**). Complete geometry optimization of **2a** showed negligible energetic effects in comparison with a  $C_s$ -constrained optimization, which was then adapted wherever possible since it enables clear state assignment.

For all of the model systems we calculated the two electromers 1-<sup>3</sup>A'' and 2-<sup>3</sup>A'', where the first possesses an Fe<sup>III</sup> ( $d^5$  configuration) with a porphyrin cation radical, and the second an Fe<sup>IV</sup> ( $d^4$  configuration) with a neutral porphyrin. The d-orbital splitting is typical of six-coordination with a "three-below-two" pattern. The lowest orbital in the group of three is the  $\delta$ -type orbital ( $d_{x^2-y^2}$ ) and the higher two are  $\pi$ -type orbitals ( $d_{xz}$  and  $d_{yz}$ ) while the group of two involves the  $\sigma$ -antibonding  $d_{z^2}$  and  $d_{xy}$  orbitals.<sup>[12]</sup> In Scheme 2 the porphyrin orbital which is singly occupied in 1-<sup>3</sup>A'' is labeled with its symmetry in the free porphyrin ( $a_{2u}$ ), as well as in its actual  $C_s$

symmetry ( $a'$ ). A 1-<sup>3</sup>A' state can be generated from 1-<sup>3</sup>A'' by switching the occupations of the  $d_{xz}$  and  $d_{yz}$  orbitals. In addition, high-spin situations ( $S=2, 3$ ), analogues of 1-<sup>3</sup>A'' and 2-<sup>3</sup>A'', were generated by excitations from the  $\pi$  and  $\delta$  d orbitals to the  $d_{z^2}$  and  $d_{xy}$  orbitals. The high-spin situations were found to be higher in energy (<sup>7</sup>A' by 4.1 kcal mol<sup>-1</sup>, <sup>5</sup>A'' by 7.9 kcal mol<sup>-1</sup>, and <sup>5</sup>A' by 19 kcal mol<sup>-1</sup>) relative to the lowest triplet state. An alternative to 1-<sup>3</sup>A'' is the triplet state, where the singly occupied porphyrin orbital<sup>[8]</sup> is  $a_{1u}$ -type ( $a''$ ). This state was tested too and found to be 16.3 kcal mol<sup>-1</sup> higher than 1-<sup>3</sup>A''. Since all these states are significantly higher than the ones shown in Scheme 2, they are not discussed any further here.

Table 1 shows relative energies and key structural parameters for the three triplet states of the ferryl-hydroxo species. It is seen that the two electromers 1-<sup>3</sup>A'' and 2-<sup>3</sup>A'' are very close in energy to within  $\pm 1$  kcal mol<sup>-1</sup>, with a small preference for one state or the other, depending on substituents, and in general agreement with a recent theoretical analysis.<sup>[13]</sup> The small substituent effect on the relative energy of the two states is in line with the size of the  $a'$  ( $a_{2u}$ ) porphyrin orbital

coefficients, which are small at the  $\alpha$ - and  $\beta$ -pyrrole positions. On the other hand, the 1-<sup>3</sup>A' state (with the  $d_{xz}^1 d_{yz}^2$  population) is significantly higher in energy, as might be expected from four-electron Pauli repulsion due to interaction of the sulfur and/or oxygen lone pairs with the filled  $d_{yz}$  orbital on iron. The Fe-O and Fe-S axial bond lengths in the 1-<sup>3</sup>A'' Por<sup>+</sup>Fe<sup>III</sup>OH state are longer than in the 2-<sup>3</sup>A'' PorFe<sup>IV</sup>OH state, a trend which is again expected from the higher Pauli repulsion between the lone pair electrons and the  $d_{yz}/d_{xz}$  electrons in the former state.

Mixing of the two <sup>3</sup>A'' states is symmetry-permitted. However, since the  $a_{2u}$  ( $a'$ ) porphyrin orbital and the  $d_{yz}$  ( $a''$ ) orbital are spatially separated and of different symmetry, the state mixing is expected to be rather small, and we may regard the two states as virtually pure ones rather than as resonance structures. To assess the barrier between the two states, which differ by single electron transfer from the iron to the porphyrin, we calculated the vertical energy separation of the two states. The vertical energy gap between 1-<sup>3</sup>A'' and 2-<sup>3</sup>A'' at the geometry of the former is 1.21 kcal mol<sup>-1</sup> for **2a**, 1.10 kcal mol<sup>-1</sup> for **2b**, and 3.48 kcal mol<sup>-1</sup> for **2c**. With such

Table 1. Bond lengths [ $\text{\AA}$ ] and relative energies  $E_{\text{rel}}$  [kcal mol<sup>-1</sup>] of the lowest states of the hydroxo-iron complex (see Scheme 2).

Species	State 1- <sup>3</sup> A'' (1- <sup>3</sup> A'), Por <sup>+</sup> Fe <sup>III</sup> OH <sup>[a]</sup>				State 2- <sup>3</sup> A'', Por Fe <sup>IV</sup> OH <sup>[a]</sup>			
	Fe-O	Fe-S	Fe-N <sup>[b]</sup>	$E_{\text{rel}}$	Fe-O	Fe-S	Fe-N <sup>[b]</sup>	$E_{\text{rel}}$
<b>2a</b>	1.829 (1.869)	2.458 (2.529)	2.017 (2.012)	0.00 (+8.67)	1.816	2.361	2.012	-0.34
<b>2b</b>	1.828 (1.870)	2.460 (2.526)	2.018 (2.013)	0.00 (+9.03)	1.817	2.362	2.013	-0.77
<b>2c</b>	1.817 (-)	2.540 (-)	2.015 (-)	0.00 (-)	1.824	2.353	2.014	+0.11
<b>2d</b>	1.810 (-)	2.530 (-)	2.015 (-)	0.00 (-)	1.808	2.336	2.009	+2.30
<b>2a<sup>[c]</sup></b>	1.829	2.458	2.017	0.00	1.816	2.361	2.012	+13.9

[a] Upon removal of the  $C_s$  constraints, the S-H and O-H bonds in the 2-<sup>3</sup>A'' structure assume a dihedral angle of 90° and the energy is lowered by 1.2 kcal mol<sup>-1</sup>. Electromer 1-<sup>3</sup>A'' is stabilized by 0.54 kcal mol<sup>-1</sup>. [b] Average value. [c] Calculated with the SCRF solvation model. Note that the bond lengths are the same as for **2a**, but the relative energies are different.

small vertical energy gaps, the two electromers are expected to be fluxional with a very small barrier for interconversion.

Since the computed dipole moment of the  $1^{-3}A''$  ( $\text{Por}^{+}\text{Fe}^{\text{III}}\text{OH}$ ) electromer (1.31 D) is larger than that of the  $2^{-3}A''$  ( $\text{PorFe}^{\text{IV}}\text{OH}$ ) electromer (1.17 D), and since the cation radical situation in the former state will endow it as well with a high polarizability, the state ordering will certainly change in the electric field environment of the protein.<sup>[14]</sup> To mimic an environment with a dielectric, we used the SCRF solvation model (with water as solvent). While this is certainly a crude model, it is nevertheless likely to reveal the expected trend in the state ordering when the states are taken from an isolated molecular situation to an environment with a finite dielectric constant. As can be seen from the last entry in Table 1, the dielectric environment stabilizes the  $1^{-3}A''$  ( $\text{Por}^{+}\text{Fe}^{\text{III}}\text{OH}$ ) electromer relative to the  $2^{-3}A''$  one, and makes it the ground state of the ferryl–hydroxo species. This result is in accord with experimental data by Groves et al.,<sup>[5]</sup> who demonstrated that the electrochemical oxidation of  $\text{PorFe}^{\text{III}}\text{OH}$  derivatives is porphyrin-centered, leading to  $\text{Por}^{+}\text{Fe}^{\text{III}}\text{OH}$ . In a condensed-phase environment we may also expect significant barriers for the interconversion of the two electromers. Analogous electromers ( $\text{Por}^{+}\text{Fe}^{\text{III}}\text{OCH}_2\text{CHPh}$  vs.  $\text{PorFe}^{\text{IV}}\text{OCH}_2\text{CHPh}$ ) have been discussed recently in the epoxidation of styrene by model iron porphyrin complexes.<sup>[15]</sup>

The electronic structure of the hydroxo–ferryl complex has bearing on the reactivity of the rebound step (Scheme 1). Inspection of Scheme 2 shows that the hydroxo–iron intermediate commences with a porphyrin hole in the  $a_{2u}$  orbital. In the alcohol product,  $\text{PorFe}^{\text{III}}\text{O}(\text{H})\text{R}$ , the porphyrin gains an electron and its  $a_{2u}$  orbital becomes doubly occupied.<sup>[8]</sup> This electron is lost from the alkyl radical, which acquires a positive oxidation state upon R–O bond formation.<sup>[16]</sup> Hence, the radical coupling will be attended by an electron shift, whereby the attacking alkyl group forms an R–O bond with concomitant loss of an electron, which is shifted to fill the porphyrin hole (in  $1^{-3}A''$ ). In the rebound step the intermediate species can couple into either a doublet ground state or a higher lying quartet state of the ferric–alcohol product (Scheme 1).<sup>[8, 17]</sup> The barrier may occur on one of these spin surfaces, or on both; this is something which has to be deciphered in a separate study.<sup>[17]</sup> Be this as it may, the rebound barrier is expected to depend inter alia on the oxidation potential of the alkyl group, and to increase as the alkyl group is made a poorer electron donor. Such a trend may provide a rationale for the observations that the hydroxylation of 1-alkyl-2-aryl-cyclopropane derivatives, which are radical-clock precursors, exhibits decreasing skeletal rearrangement in the alcohol product as the putative radical intermediate becomes a better electron donor.<sup>[3]</sup>

A theoretical investigation of the entire rebound process in the electric field of the protein will be required<sup>[18]</sup> for a more complete elucidation of the rebound mechanism. Nevertheless, with its obvious limitations, the present study provides straightforward characterization of the electronic structure of the putative intermediate in the mechanisms as well as of the electron transfer attending the rebound step, and can thereby form a basis for experimental investigation of the rebound step. Substituted iron porphyrin derivatives,<sup>[19]</sup> different axial

ligands,<sup>[15]</sup> medium effect, and different radical probes can provide a powerful mechanistic arsenal towards this goal.

Received: June 11, 1999 [Z13547IE]

German version: *Angew. Chem.* **1999**, *111*, 3730–3733

**Keywords:** alkane hydroxylations • C–H activation • cytochrome P450 • density functional calculations • enzyme catalysis

- [1] a) M. Sono, M. P. Roach, E. D. Coulter, J. H. Dawson, *Chem. Rev.* **1996**, *96*, 2841; b) W.-D. Woggon, *Top. Curr. Chem.* **1996**, *184*, 40.
- [2] J. T. Groves, *J. Chem. Educ.* **1985**, *62*, 928.
- [3] P. H. Toy, M. Newcomb, P. F. Hollenberg, *J. Am. Chem. Soc.* **1998**, *120*, 7719.
- [4] a) J. T. Groves, Y.-Z. Hang in *Cytochrome P450: Structure, Mechanisms and Biochemistry* (Ed.: P. R. Ortiz de Montellano), 2nd ed., Plenum, New York, **1995**, chap. 1; b) J. I. Manchester, J. P. Dinnocenzo, L. A. Higgins, J. P. Jones, *J. Am. Chem. Soc.* **1997**, *119*, 5069; c) recent findings (Y. Goto, Y. Watanabe, S. Fukuzumi, J. P. Jones, J. P. Dinnocenzo, *J. Am. Chem. Soc.* **1998**, *120*, 10762) show that some dimethylaniline derivatives are oxidized by an electron transfer mechanism. However, this is not relevant for substrates which undergo benzylic C–H hydroxylation (cf. ref. [4b]). For these substrates the equality of the isotope effects of the P450 oxidation with those in the hydrogen abstraction by  $t\text{BuO}^{\bullet}$  still demonstrates that the transition states in P450 hydroxylation bear resemblance to transition states of a hydrogen-abstraction reaction.
- [5] J. T. Groves, Z. Gross, M. K. Stern, *Inorg. Chem.* **1994**, *33*, 5065.
- [6] Electromers are electronic isomers which possess the same atom connectivity, but differ in their electron occupation. For a discussion of this term and its historic connotation, see: H. Zuilhoff, J. P. Dinnocenzo, A. C. Reddy, S. Shaik, *J. Phys. Chem.* **1996**, *100*, 15774.
- [7] a) A. Wolberg, J. Manassen, *J. Am. Chem. Soc.* **1970**, *92*, 2982; b) R. H. Felton, G. S. Owen, D. Dolphin, J. Fajer, *J. Am. Chem. Soc.* **1971**, *93*, 6332; c) P. Gans, G. Buisson, E. Duee, J.-C. Marchon, B. S. Erler, W. F. Scholz, C. A. Reed, *J. Am. Chem. Soc.* **1986**, *108*, 1223.
- [8] M. Filatov, N. Harris, S. Shaik, *J. Chem. Soc. Perkin Trans. 2* **1999**, 399.
- [9] JAGUAR 3.5, Schrodinger, Inc, Portland, OR, **1998**.
- [10] a) A. D. Becke, *Phys. Rev. A* **1988**, *38*, 3098; J. P. Perdew, *Phys. Rev. B* **1986**, *33*, 8822; b) P. J. Stevens, F. J. Devlin, C. F. Chabrowski, M. J. Frisch, *J. Phys. Chem.* **1994**, *98*, 11623.
- [11] LACVP: J. P. Hay, W. R. Wadt, *J. Chem. Phys.* **1985**, *82*, 299. LACV3P is a triple-zeta contraction of LACVP tested in ref. [9].
- [12] A d-block diagram used often in the literature involves a coordinate system where the  $x$  and  $y$  axes pass through the nitrogen atoms of the porphyrin ring. This diagram switches the labels of the  $d_{x^2-y^2}$  and  $d_{xy}$  orbitals relative to their ordering in Scheme 2. Recall, however, that in any coordinate system, the lowest orbital is  $\delta$  type followed by two  $\pi$  types. The higher lying orbitals are  $\sigma^*$  types, one ( $d_z$ ) along the  $z$  axis and the other (either  $d_{xy}$  or  $d_{x^2-y^2}$  depending on the coordinate system) in the porphyrin plane.
- [13] D. H. Jones, A. S. Hinman, T. Ziegler, *Inorg. Chem.* **1993**, *32*, 2092.
- [14] D. Harris, G. H. Loew, *J. Am. Chem. Soc.* **1993**, *115*, 8775.
- [15] Z. Gross, S. Nimri, C. M. Barzilay, *J. Bioinorg. Chem.* **1997**, *2*, 492.
- [16] The electron which fills the porphyrin hole must be supplied by the R–O linkage, since the oxygen atom in  $1^{-3}A''$  is already saturated, having one bond to the iron and another bond to hydrogen. Following the oxidation state formalism, this electron comes from the alkyl group.
- [17] N. Harris, S. Cohen, M. Filatov, F. Ogliaro, S. Shaik, unpublished results.
- [18] H. Aissaoui, R. Bachmann, A. Schweiger, W.-D. Woggon, *Angew. Chem.* **1998**, *110*, 3191; *Angew. Chem. Int. Ed.* **1998**, *37*, 2998.
- [19] D. Dolphin, T. G. Traylor, L. Y. Xie, *Acc. Chem. Res.* **1997**, *30*, 251.